GEOPHYSICS, VOL. 72, NO. 2 (MARCH-APRIL 2007); P. E77–E86, 10 FIGS., 1 TABLE.
10.1190/1.2431636

Seismic signatures of partial saturation on acoustic borehole modes

Gabriel Chao[1], D. M. J. Smeulders[1], and M. E. H. van Dongen[2]

ABSTRACT

We present an exact theory of attenuation and dispersion of borehole Stoneley waves propagating along porous rocks containing spherical gas bubbles by using the Biot theory. An effective frequency-dependent fluid bulk modulus is introduced to describe the dynamic (oscillatory) behavior of the gas bubbles. The model includes viscous, thermal, and radiation damping. It is assumed that the gas pockets are larger than the pore size, but smaller than the wavelengths involved (mesoscopic inhomogeneity). A strong dependence of the attenuation of the Stoneley wave on gas fraction and bubble size is found. Attenuation increases with gas fraction over the complete range of studied frequencies (10 Hz–50 kHz). The dependence of the phase velocity on the gas fraction and bubble size is restricted to the lower frequency range. These results indicate that the interpretation of Stoneley wave properties for the determination of, for example, local permeability formation is not straightforward and could be influenced by the presence of gas in the near-wellbore zone. When mud-cake effects are included in the model, the same observations roughly hold, though dependence on the mud-cake stiffness is quite complex. In this case, a clear increase of the damping coefficient with saturation is predicted only at relatively high frequencies.

INTRODUCTION

One of the main objectives of logging techniques is to determine the volume fraction of the fluids saturating the pore space of a reservoir. Oil, water, and gas commonly coexist in prospective reservoirs, and an accurate assessment of oil content is needed to assert the economic value of the reservoir. It is common practice to estimate oil saturation from resistivity logs by means of semiquantitative methods based on the empirical formula postulated by Archie (1942), (see, e.g., Hearst et al., 2000). These models incorporate conductivity effects in rocks with high clay content such as shaley sands (Waxman and Smits, 1968; Clavier et al., 1984; Sen and Goode, 1988). Saturation also affects acoustics. In particular, changes in the compressibility of the reservoir affect damping of the seismic waves because of the additional mesoscopic damping mechanisms (see, e.g., Pride et al., 2003). Therefore, acoustic logging surveys provide insight-yielding information complementary to the more commonly employed resistivity logs.

Acoustic borehole methods have evolved rapidly since the early times when only information about porosity and elastic velocities in the formation were obtained through identification of the distinct arrivals of head waves. In recent years, there has been an increasing interest in the interpretation of full-waveform acoustic logs in order to characterize poroelastic properties of the reservoir and the saturating fluid (see, e.g., White, 1983; Paillet and Cheng, 1991; Tang and Cheng, 2004). The emphasis of these investigations was directed toward understanding the relationship between permeability and dispersive velocity and attenuation of the Stoneley wave propagating along the borehole (Rosenbaum, 1974; Schmitt et al., 1988; Winkler et al., 1989; Tang and Cheng, 1996; Chao et al., 2004). From these theoretical and experimental studies, it has become obvious that a strong dependence of the attenuation of the Stoneley wave on permeability can be expected, though other dissipative mechanisms can influence the propagation of this surface wave. From a practical point of view, it is important to consider the influence of the mud-cake layer that forms against the borehole wall during drilling. The mud cake imposes restrictions to the exchange of flow between the borehole and pore fluid, therefore reducing the sensitivity of the Stoneley wave to the poromechanical properties of the formation.

The purpose of this work is to study the influence of relatively small amounts of gas on the features of the Stoneley wave in liquid-saturated formations. It is not our aim to propose a method to determine liquid saturation from acoustic logs, but to understand the physical mechanisms that govern the propagation of the Stoneley wave along boreholes in partially saturated reservoirs. We assume that the reservoir is saturated by a liquid-gas mixture. The study of saturation effects on the properties of body waves has received considerable attention since the pioneering paper of White (1975). The

Manuscript received by the Editor February 1, 2006; revised manuscript received September 20, 2006; published online February 9, 2007.
[1]Delft University of Technology, Department of Geotechnology, Delft, the Netherlands. E-mail: g.e.chao@tue.nl; d.m.j.smeulders@citg.tudelft.nl.
[2]Eindhoven University of Technology, Department of Applied Physics, Eindhoven, the Netherlands. E-mail: m.e.h.v.dongen@tue.nl.

White model assumes that gas fraction is constituted as spherical gas pockets distributed in a cubic array in the liquid-saturated porous medium. Dutta and Ode (1979a, b) provided a more complete solution based on Biot's (1956a, b) theory for the bulk modulus of a single bubble surrounded by a spherical liquid-saturated porous medium. In this work, we describe the acoustic bulk properties of the partially saturated reservoir according to the model proposed by Smeulders and van Dongen (1997). Their model is based on the response of a gas bubble in a fully saturated Biot medium to an external oscillating pressure field. In many respects this formulation resembles the original White-Dutta-Ode model, but it also incorporates damping mechanisms caused by heat exchange between the gas phase and the solid matrix. Moreover, it allows for the existence of a propagating slow wave that is vital for the correct description of surface waves.

There has been no analysis so far concerning the influence of liquid saturation on the Stoneley wave in borehole configurations. Numerical results for plane geometries are reported by Chao et al. (2006a). We extend these calculations to cylindrical geometries. Frequency-dependent properties of the Stoneley wave are investigated in the complete seismic and borehole band of frequencies (10 Hz–50 kHz). We study the sensitivity of the phase velocity and attenuation of the Stoneley wave to variations of the gas fraction. As a first attempt to model the complicated boundary between borehole fluid and the partially saturated formation, the model allows for the existence of an elastic mud cake of negligible thickness. Other models also considered the influence of the flushed and transition zones (Han and Batzle, 1997).

We will analyze the numerical results for the phase velocity and damping coefficient of the Stoneley wave for several values. This will be followed by analysis of the influence of the gas bubble radii on frequency-dependent speed and attenuation at a fixed liquid saturation. At a given frequency, we study the pore-pressure radial distribution induced by the Stoneley wave for different liquid saturations. Thereafter we analyze quantitatively the sensitivity of both the phase velocity and damping coefficient of the Stoneley wave to the gas fraction in the pore space. Subsequently, the influence of a mud-cake layer will be investigated.

BOREHOLE WAVES IN PARTIALLY SATURATED POROUS MEDIA

We consider a borehole in a partially saturated porous formation. The configuration is presented schematically in Figure 1. Material physical properties of the poroelastic formation (Table 1) have been taken from Carcione et al. (2003). They correspond to a solid matrix consisting of a mixture of 90% quartz and 10% clay; the saturating liquid is brine. The properties of the gas phase are chosen to simulate actual reservoir conditions. The bulk acoustic properties of the reservoir saturated by the mixture of brine and gas are described according to the formulation outlined in Appendix A (Smeulders and van Dongen, 1997). It is assumed that the gas volumes are homogeneously distributed and that they are within a very narrow range of bubble radii. The bubble radius is larger than the grain size but smaller than the wavelengths involved; therefore, we assume the fluid mixture to be homogeneous. The model is based on the calculation of the volume variation of a single bubble as a response to a harmonic pressure field. The dynamics of the bubble are determined by the solution of Biot equations at the spherical interface between gas-saturated and brine-saturated porous media. Mathematically, we solve the Biot equations in spherical coordinates both inside and outside the bubble. The solutions are then matched by using appropriate boundary conditions, and the bubble-volume change caused by harmonic pressure can be calculated. In this way, the bulk modulus of the bubble can be computed. Neglecting the interaction between different bubbles, this bulk modulus can be considered as the effective bulk modulus of the gas phase $K_g(\omega)$ in the gas-liquid mixture. The frequency-dependent bulk modulus of the mixture $K_f(\omega)$ is obtained through a frequency-dependent Wood's formula (Wood, 1955):

$$\frac{1}{K_f(\omega)} = \frac{s}{K_l} + \frac{1-s}{K_g(\omega)}, \tag{1}$$

where K_l is the bulk modulus of the liquid phase and s is the brine saturation. The resulting compressibility plots are given in Figure 2.

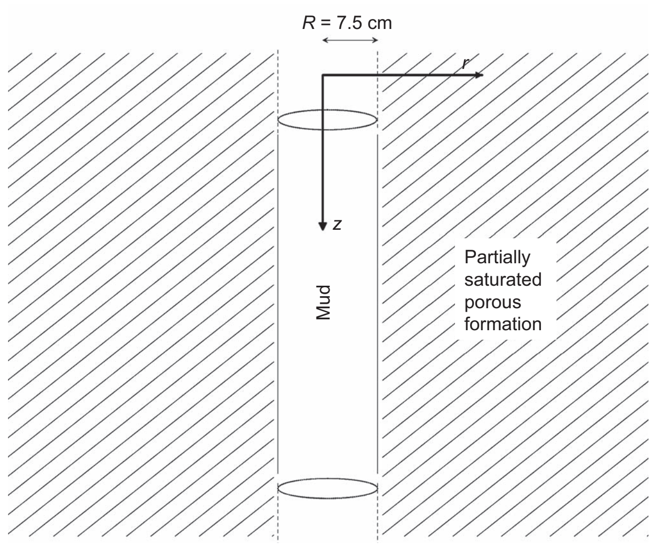

Figure 1. Borehole in a partially saturated reservoir. Properties of the formation are given in Table 1. The reservoir is saturated with a homogeneous brine-gas mixture.

Table 1. Physical properties of the rock and saturating fluids.

Solid density ρ_s (kg/m^3)	2585
Porosity ϕ	0.3
Permeability k_0 (D)	0.55
Tortuosity α_∞	2.5
Frame bulk modulus K_b (GPa)	8.67
Shear modulus N (GPa)	6.61
Solid-grain bulk modulus K_s (GPa)	34.3
Brine bulk modulus K_l (GPa)	2.4
Brine density ρ_l (kg/m^3)	1040
Brine viscosity η_l (mPa s)	1.8
Gas pressure p_g (GPa)	0.01
Gas density ρ_g (kg/m^3)	100
Gas viscosity η_g(mPa s)	0.02
Gas thermal diffusivity a_g (m^2/s)	1.87×10^{-7}
Gas polyatomic constant γ	1.4

The data are normalized to the bulk modulus of the liquid.

Because the Stoneley wave can be expressed as a superposition of the different bulk waves, it is illustrative to examine the features of these waves in a partially saturated porous medium. To obtain the dispersive phase velocities and attenuations of the body waves, we couple the classical Biot equations

$$-\omega^2(\tilde{\rho}_{11}\mathbf{u} + \tilde{\rho}_{12}\mathbf{U}) = (P - N)\nabla\nabla \cdot \mathbf{u} + N\nabla^2\mathbf{u} + Q\nabla\nabla \cdot \mathbf{U} \quad (2)$$

and

$$-\omega^2(\tilde{\rho}_{22}\mathbf{U} + \tilde{\rho}_{12}\mathbf{u}) = R\nabla\nabla \cdot \mathbf{U} + Q\nabla\nabla \cdot \mathbf{u}, \quad (3)$$

with the aforementioned description for the bulk modulus of the gas-liquid mixture (equation 1 and Appendix A). In equations 2 and 3, $\mathbf{u}$ is the solid displacement and $\mathbf{U}$ is the fluid displacement. The shear modulus of the composite material is N, and P, Q, and R are the so-called generalized elastic coefficients. They are related to the porosity ϕ, the solid-frame bulk modulus K_b, the solid-grain bulk modulus K_s, the pore-fluid modulii K_f and N through so-called Gedanken experiments (see, e.g., Allard, 1993). The $F(\omega)$ operator describes the frequency-dependent interaction between the solid matrix and the fluids filling the void space. The most remarkable result of this theory is the accurate prediction of an extra compressional wave, commonly called the Biot slow P-wave. This wave is characterized by an out-of-phase movement between solid and liquid phases. It presents a strong frequency-dependent behavior and is diffusive at low frequencies where the viscous effects dominate and propagative at high frequencies. The transition between these two regimes is distinguished by the so-called critical frequency f_c:

$$f_c = \frac{\eta\phi}{2\pi\kappa_0\alpha_\infty\rho_f}, \quad (4)$$

where η is the effective viscosity of the fluid phase, κ_0 the steady-state permeability, α_∞ is the tortuosity of the medium, and ρ_∞ the effective density of the fluid phase. Figure 3 shows the phase velocities and damping coefficients of the three bulk modes that propagate through the formation characterized by the properties listed in Table 1. Two scenarios are considered: (1) a fully saturated formation and (2) a partially saturated porous medium with a liquid saturation of 0.95 and a bubble radius of 1 mm. The size of the gas bubbles was taken in accordance with values reported in Dutta and Ode (1979b), Carcione et al. (2003), Taylor and Knight (2003), and Pride et al. (2004). The decrease in the bulk modulus of the mixture caused by the presence of gas bubbles results in slower propagation of compressional waves in the partially saturated case than in the fully saturated medium. Also, oscillations of the bubbles induce energy loss in compressional waves, as can clearly be observed in Figure 3b. It is worthwhile to mention that similar results can be obtained by using the classical White-Dutta-Ode model (Dutta and Ode, 1979a, b).

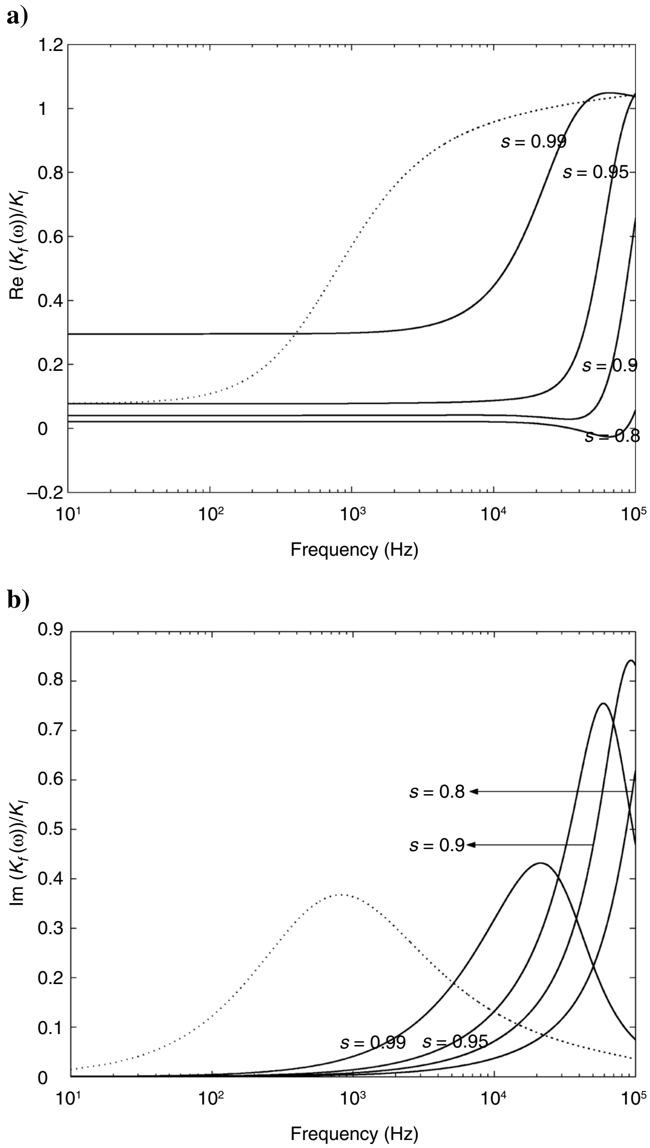

Figure 2. Frequency-dependent bulk modulus of the brine-gas mixture. (a) The real part accounts for the compressibility of the system and (b) the imaginary part renders the loss mechanisms. Bubble radius is 1 mm. Computations for a bubble radius of 1 cm and brine saturation $s = 0.95$ are shown as a dotted line.

Dispersive borehole modes are obtained by solving a boundary-value problem in the frequency domain. The different bulk modes in the poroelastic formation and the borehole fluid are coupled through the boundary conditions. Mathematically, this coupling leads to an implicit relationship between the wavenumber and the frequency, which is solved numerically by using a zero search routine in the complex plane (see, e.g., Chao et al., 2004; Liu, 1988; Winkler et al., 1989). There are an infinite number of surface waves that can propagate in borehole geometries (see, e.g., Chao et al., 2006b; Sinha and Asvadurov, 2004). In this investigation, we restrict ourselves to the fundamental mode, the Stoneley wave, which at low frequencies is usually referred to as the tube wave. Figure 4 displays the phase velocities and damping coefficients of the Stoneley wave as a function of frequency for different brine saturations s. The phase velocity shows a strong dependence on brine saturation at low frequencies. Because of compressibility effects, the phase velocity decreases with decreasing saturation in the low-frequency range (10 Hz–5 kHz). This dependence is reversed at higher frequencies where loss mechanisms induced by gas bubble oscillations become significant. The damping coefficient in Figure 4b is expressed as the imaginary part of the complex-valued wavenumber of the Stoneley wave. Our numerical calculations predict a significant dependence on the brine saturation. Attenuation increases with decreasing brine saturation over the complete range of frequencies (10 Hz–50 kHz).

Frequencies involved in acoustic borehole logging range from several hundred hertz to 30 kHz. The effect of saturation on the damping coefficient in this band of frequencies is significant. Values of the damping coefficient for representative frequencies of 2, 7.5, 10, and 20 kHz are depicted in Figure 5. We obtain discrepancies of an approximate factor of two when a gas fraction of 1% is introduced. These results suggest that the attenuation of the Stoneley wave is highly sensitive to the gas fraction in the pore space. A comparison of the effects of changes in liquid saturations on the attenuations of the Stoneley waves and P-waves reveals no significant qualitative differences. Obviously, the levels of attenuation for the Stoneley wave are higher because of the oscillating fluid flow at the borehole wall. These arguments seem to indicate that, at least in our simplified model, the dependence of attenuation on brine saturation is mainly caused by compressibility changes rather than interfacial dissipative mechanisms.

In order to explain the frequency-dependent behavior of phase velocity and damping coefficient and their relationship to liquid saturation, it is illustrative to examine the complex-valued, frequency-dependent bulk modulus of the mixture saturating the pore space of the porous medium. The complex-valued bulk modulus is depicted in Figure 2. The real part accounts for the compressibility of the mixture, and the imaginary part reflects the loss mechanisms induced by oscillations of gas bubbles. For low frequencies, the real part is frequency independent and can be obtained by a simple average of the liquid and the gas steady-state bulk moduli. At these frequencies, it is also obvious, from Figure 2b, that the dissipative mechanisms induced by oscillations of gas bubbles are inactive; therefore, only compressibility effects are responsible for the change of the proper-

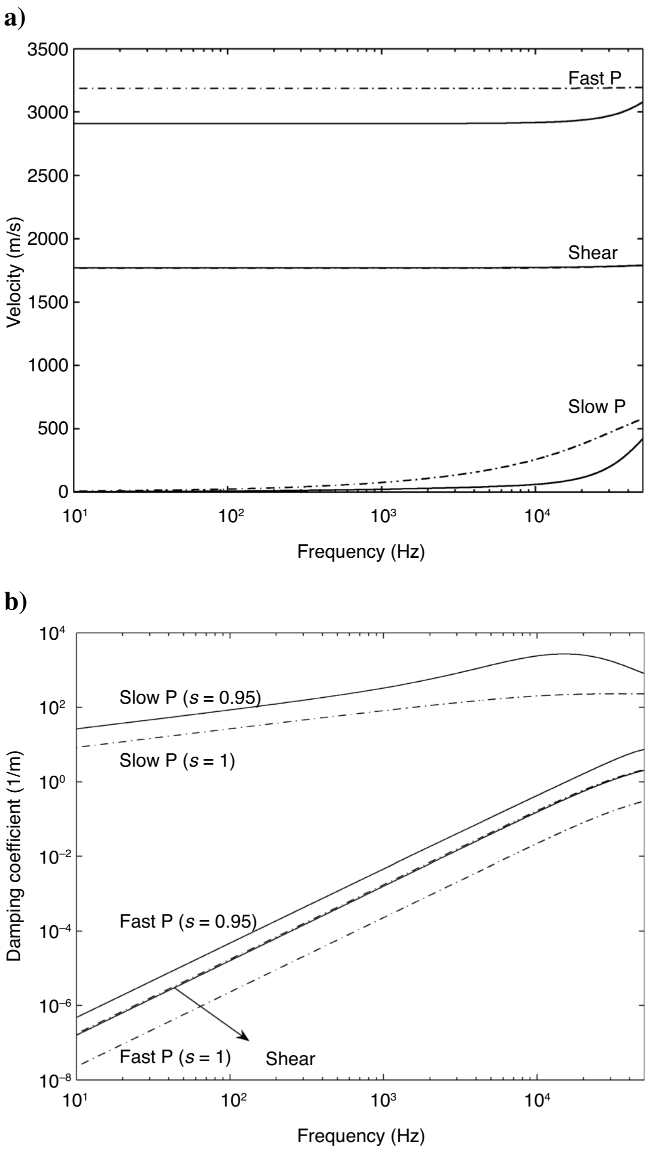

Figure 3. (a) Phase velocities and (b) damping coefficients of the body waves propagating in a brine-gas–saturated sandstone. The damping coefficient is defined as the imaginary part of the complex-valued wavenumber. Effects of gas saturation are shown as solid lines, gas pressure is 0.01 GPa, bubble radius is 1 mm, and brine saturation is 0.95. Biot predictions for the fully saturated reservoir are shown as dotted lines.

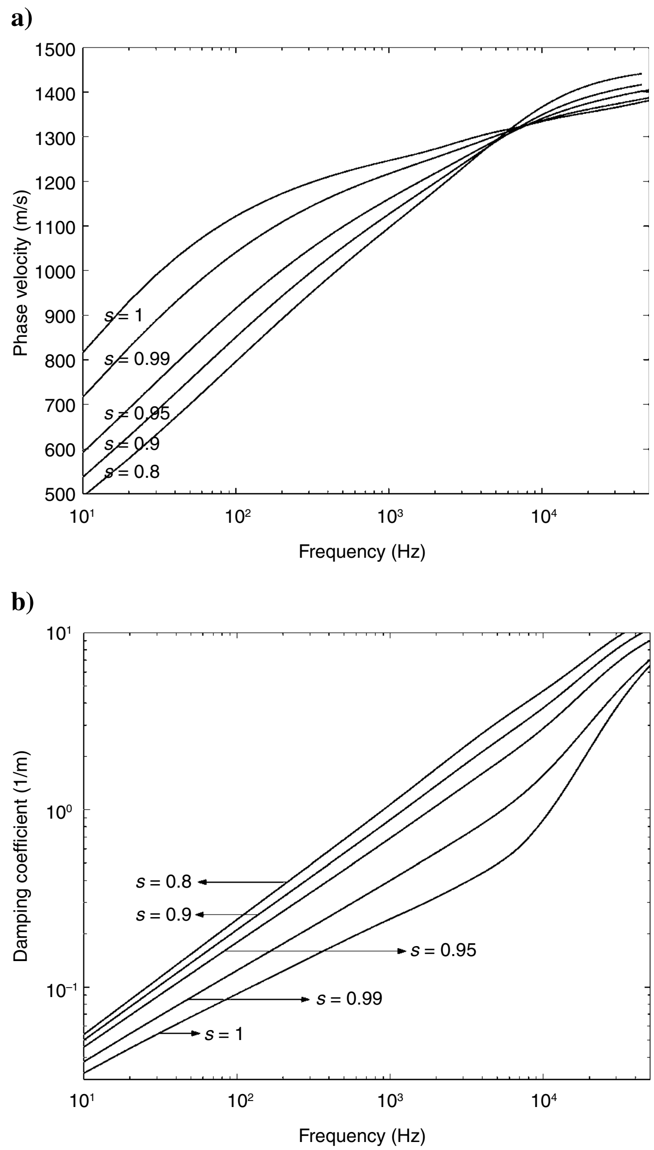

Figure 4. (a) Frequency-dependent phase velocity and (b) damping coefficient of the Stoneley wave for different values of brine saturation *s*.

ties of the Stoneley wave with respect to the fully saturated case. As the frequency is increased, an important decrease of compressibility is observed. The damping mechanisms also become important. We note that for frequencies below 30 kHz, the bulk loss mechanisms decrease with increasing gas fraction. However, the damping coefficient of the Stoneley wave increases significantly with increasing gas volume. It is evident that propagation of the Stoneley wave is mainly governed by the frequency-dependent compressibility of the mixture. In spite of the fact that the loss mechanisms may have an influence on the Stoneley wave, it is obvious that they are not responsible for the clear trend found in the damping coefficient.

The bubble radius is a critical parameter that conditions the bubble dynamics and therefore the acoustic properties of the partially saturated porous medium. We analyze the influence of the bubble radius on the Stoneley wave. Figure 6 shows calculations for phase velocity and the damping coefficient for two bubble radii. For comparison, the dispersion curves for the fully brine-saturated case are shown in dashed lines. We observe that by increasing the radius of the bubbles, dependence on saturation decreases drastically and is restricted to the low-frequency part of the spectrum. With the aid of Figure 2a, we can conclude that, because of the increase of compressibility of the mixture when larger bubbles are considered, the range of frequencies at which saturation influences the Stoneley wave is restricted to those where the contrast of compressibility is significant. We should mention that considering a single value for the bubble radii throughout the formation seems to be unrealistic. However, for a bubble size distribution, say Gaussian, our results can easily be generalized.

Next, we examine radial penetration in the porous formation of the Stoneley wave. We compute the pore pressure as a function of the radial coordinate for different liquid saturations. We restrict our analysis to representative frequencies of 2 and 10 kHz. The results are displayed in Figure 7. The fact that radial penetration decreases with decreasing brine saturation can be explained by taking into account that the radial penetration is inversely proportional to the compressibility of the mixture. Figure 2a shows that, at these frequencies, the real part of the bulk modulus of the mixture increases with brine saturation; therefore, the compressibility decreases. We next analyze the sensitivity of the phase velocity and the damping coefficient to the variation of liquid saturation. To obtain a quantitative estimate of sensitivity, we compute the following quantities:

$$\varsigma_v = \frac{s}{v}\frac{\partial v}{\partial s} \tag{5}$$

and

$$\varsigma_D = \frac{s}{D}\frac{\partial D}{\partial s}, \tag{6}$$

where ς_v and ς_D are the sensitivity parameters, also called normalized partial derivatives (Cheng et al., 1982), and v and D are the phase velocity and the damping coefficient of the Stoneley wave, respectively. We conduct this analysis at frequencies of 2 and 10 kHz and for permeability values of 0.55 D and 5.5 mD. These permeabil-

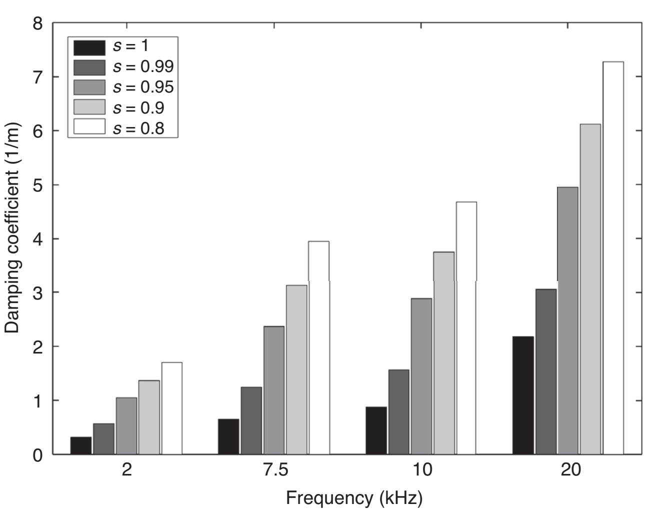

Figure 5. Damping coefficients of the Stoneley wave for different saturations at representative frequencies.

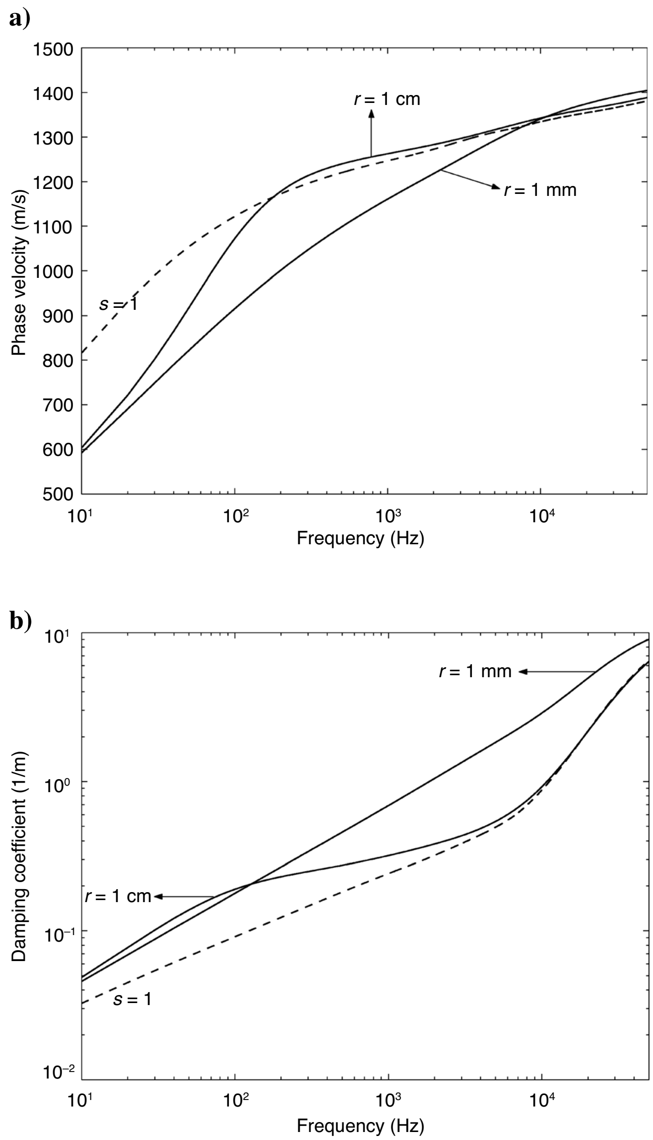

Figure 6. (a) Phase velocity and (b) damping coefficient of the Stoneley wave in a partially saturated formation. Brine saturation is $s = 0.95$. Different bubble radii (r) are considered. The solution for $s = 1$ (fully brine-saturated reservoir) is displayed, for comparison, in dashed lines.

ity values are consistent with previous studies by Dutta and Ode (1979b), Carcione et al. (2003), and Pride et al. (2004); 1 D, 0.55 D, and 10 mD, respectively. Figure 8 shows the results. The sensitivity of the damping coefficient increases monotonically with liquid saturation, and the damping coefficient is highly sensitive to this parameter, especially at very low gas concentrations; this relationship holds for both values of permeability. The method predicts a higher sensitivity for the more permeable reservoir (see Figure 8a), where this parameter presents no significant difference for the frequencies considered in this study. The phase velocity is less sensitive in both scenarios, though a sharp increase for low gas fractions in the more permeable formation is found for the 10-kHz analysis. These calculations indicate that an accurate determination of the damping coefficient can provide useful information regarding saturation of the reservoir; similar conclusions can be drawn from the analysis of the sensitivity results for the lower-permeability reservoir (5.5 mD). In this case, sensitivity of the damping coefficient increases with liquid saturation, whereas phase velocity shows a relatively low sensitivity to saturation for the frequencies considered in this study.

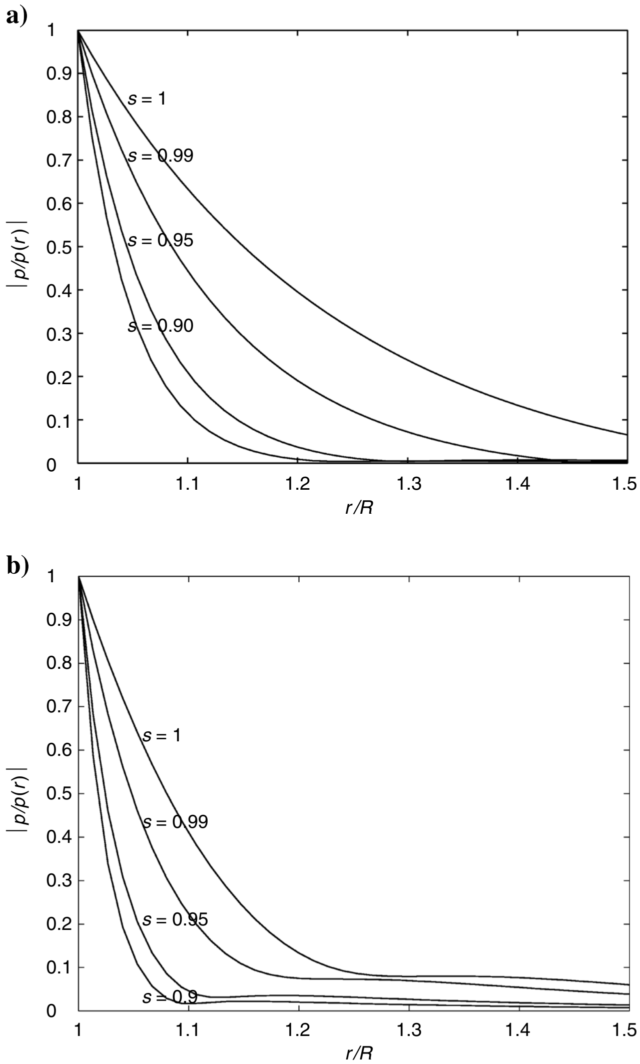

Figure 7. Pore-pressure radial distribution induced by the Stoneley wave for different brine saturations at representatives frequencies of (a) 2 and (b) 10 kHz.

MUD-CAKE EFFECTS

A complicating factor in interpreting borehole acoustic logging data is the presence of a mud-cake layer that forms against the borehole wall. This elastic structure deforms during the passage of the Stoneley wave and reduces the surface permeability of the borehole wall by partially sealing the pores at the interface. The elastic deformation is controlled by the stiffness of the mud cake, whereas the influence of the mud cake on the flow is determined by the mud-cake permeability and thickness. The influence of such a layer on the acoustic properties of the Stoneley wave has been studied by Schmitt (1988), Tang (1994), (X. M. Tang and R. J. Martin (1994), Gas Res. Inst., contract 5093-260-2753), and Liu and Johnson (1997). Schmitt (1988) modeled the mud-cake layer as a permeable poroelastic solid with a given permeability whereas Liu and Johnson

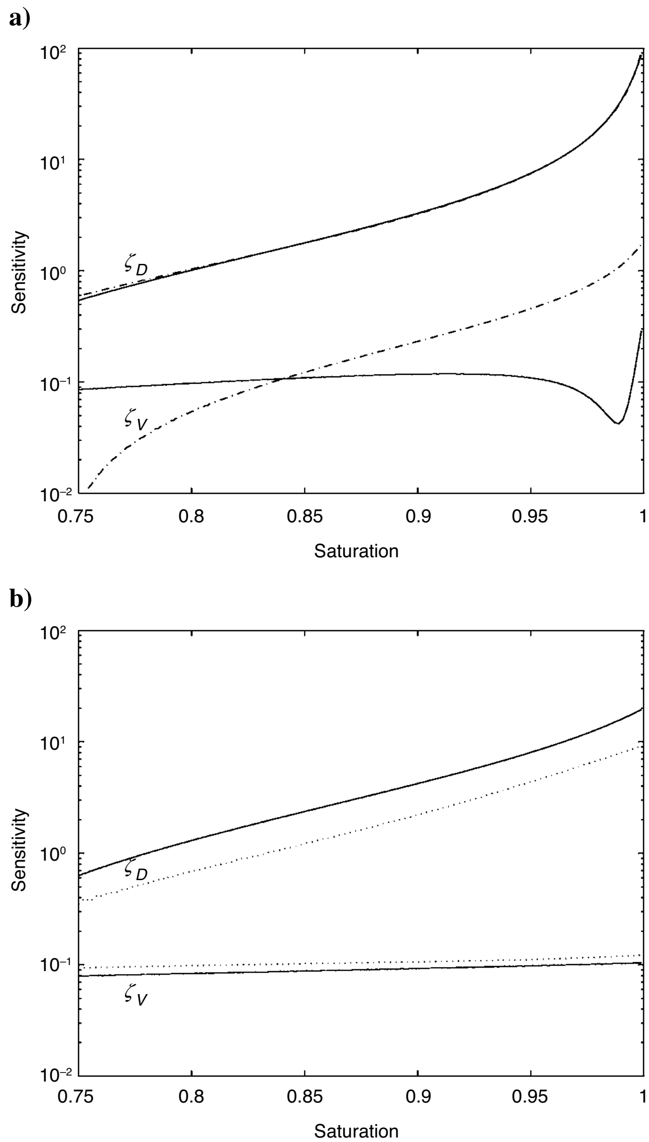

Figure 8. Sensitivity analysis of saturation for the phase velocity and damping coefficient at representative frequencies of 10 (solid lines) and 2 kHz (dashed lines). Different values for permeability, (a) k_0 = 0.55 D and (b) k_0 = 5.50 mD, are considered. The rest of the formation parameters are listed in Table 1.

(1997) assumed the mud cake to be elastic and impermeable; both investigations considered the effects of mud-cake thickness. In this work we consider the mud cake to be elastic, but of negligible width. In this way, the mud cake enters our model as a frequency-independent surface permeability of the borehole wall. The concept of surface permeability, first introduced by Deresiewicz and Skalak (1963), can be employed to model different discontinuities that may arise at the borehole wall, for example an impairment layer (see Tichelaar et al., 1999). In fact, we model the mud cake in the same way as Liu and Johnson (1997), when the width is neglected in their model (see equation 9 of Liu and Johnson, 1997):

$$P_0 - P_1 = W_{\mathrm{mc}}\phi(U_{r1} - u_{r1}), \tag{7}$$

where P stands for pressure amplitude, W_{mc} is the stiffness of the mud cake, ϕ is the porosity, U_r is the radial displacement of the fluid mixture, and u_r is the radial displacement of the solid phase. The subscript 1 denotes the porous formation; 0 refers to the borehole liquid. Tang (1994) suggested that W_{mc} is related to the mud-cake shear rigidity and the pore size in the reservoir. X. M. Tang and R. J. Martin (1994), Gas Res. Inst., contract 5093-260-2753, showed that an extremely stiff mud cake may impose restrictions to the delineation of permeability from Stoneley wave data. On the other hand, the numerical results published by Liu and Johnson (1997) suggest that the mud cake reduces, but does not eliminate, permeability effects on Stoneley wave characteristics.

The purpose of our calculations is to assess whether the presence of the mud-cake layer hampers the sensitivity of the damping of the Stoneley wave on saturation of the formation. We considered three different values for the stiffness of the mud cake (1) a soft mud cake, W_{mc} = 100 GPa/m, (2) an average mud cake, W_{mc} = 500 GPa/m, and (3) a hard mud cake, W_{mc} = 1000 GPa/m. Brine saturation values of 1 and 0.95 were considered. The results are displayed in Figures 9 and 10. At low frequencies, the mud cake shields the damping caused by wave-induced oscillating flow at the borehole wall; thus, the damping coefficient decreases for increasing W_{mc}. This shielding mechanism is more effective when there is gas in the pores, so for high W_{mc} values, damping of the Stoneley wave in the partially saturated medium may become less than in the fully saturated reservoir. This observation is no longer generally true for higher frequencies. As frequencies increase, a mud cake that gradually becomes less permeable and stiffer results in higher attenuation values in the partially saturated reservoir with respect to the fully saturated formation. This trend is observed in the open-borehole situation (W_{mc} = 0), which indicates that at these frequencies, compressibility effects prevail over flow-exchange mechanisms at the borehole wall. In the high-frequency limit, the Stoneley wave along a borehole wall behaves as the pseudo–Stoneley wave in a flat liquid/porous interface, which propagates more slowly when the interface is fully impermeable (Feng and Johnson, 1983; Gubaidullin et al., 2004). Results for the fully saturated reservoir are consistent with the numerical results by Liu and Johnson (1997).

In general, we can conclude that a clear dependence of the damping coefficient on saturation is found even in the presence of a mud-cake layer, although for stiff mud cakes having low permeabilities

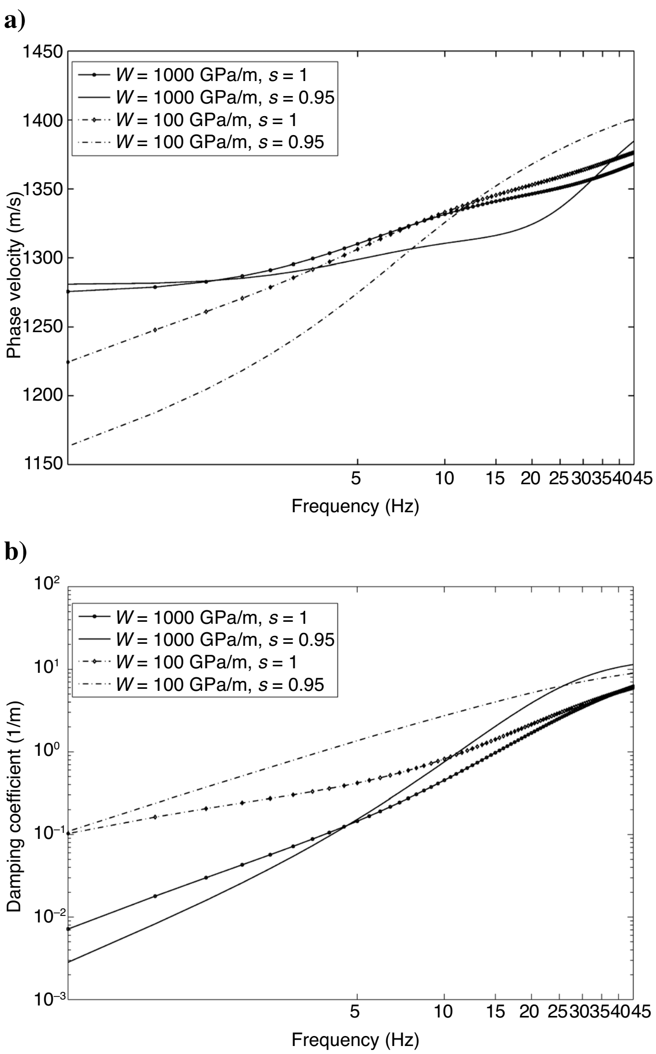

Figure 9. Saturation effects on (a) the phase velocity and (b) damping coefficient of the Stoneley wave when an elastic mud cake is present. Different values of mud-cake stiffness are considered $W_{\mathrm{mc}}^{\mathrm{soft}}$ = 100 GPa/m and $W_{\mathrm{mc}}^{\mathrm{hard}}$ = 1000 GPa/m.

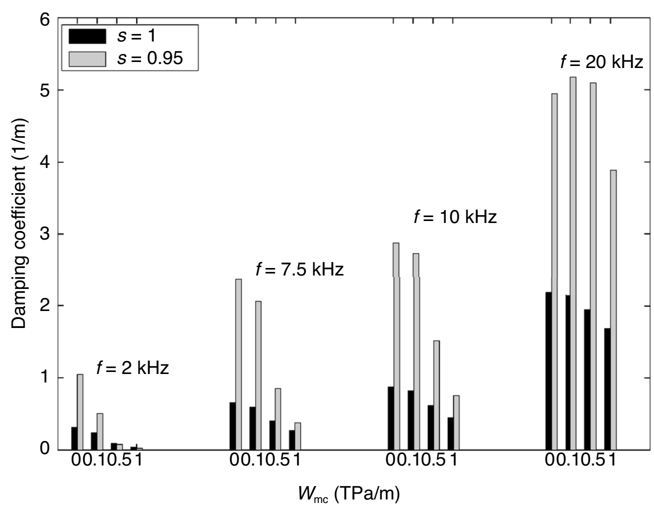

Figure 10. Damping coefficients of the Stoneley wave at representative frequencies and different stiffnesses of the mud cake $W_{\mathrm{mc}}^{\mathrm{soft}}$ = 100 GPa/m, $W_{\mathrm{mc}}^{\mathrm{average}}$ = 500 GPa/m, and $W_{\mathrm{mc}}^{\mathrm{hard}}$ = 1000 GPa/m. W_{mc} = 0 corresponds to the open-pore boundary condition, i.e., a condition with no mud cake.

and at low frequencies, the combined effects of the mud cake and the gas may interfere so that no net effect can be discerned.

CONCLUSIONS

This study reports numerical results on the influence of gas fraction on propagation of the Stoneley wave along a borehole surrounded by a partially saturated poroelastic formation.

Our results indicate that there is a strong dependence of phase velocity and damping coefficient on the liquid saturation in the porous reservoir. The damping coefficient shows a clear increase with increasing gas fraction throughout the band of frequencies studied (10 Hz–50 kHz). The dependence of phase velocity on liquid saturation is restricted to low frequencies. The frequency-dependent properties of the phase velocities and damping coefficients — and the dependence of those properties on the gas fraction — can be explained in terms of compressibility variations in the mixture caused by the presence of gas volume.

The outcome of these investigations suggests that information regarding the saturation of a porous reservoir can be inferred through analysis of the damping coefficient of the Stoneley wave. Remarkably, in the band of frequencies related to borehole acoustics techniques, the variation and sensitivity of the damping coefficient to changes in saturation are quite appreciable. One complicating factor in interpreting the results is the presence of a mud cake that severely hampers the borehole-reservoir fluid connectivity. Our numerical results indicate that the high-frequency band of the Stoneley wave spectrum may provide better information on reservoir saturation when stiff mud cakes are present.

ACKNOWLEDGMENTS

This study was financially supported by the ISES (Integrated Solid Earth Sciences) program. We thank anonymous reviewers for useful comments that helped to improve the quality of the manuscript.

APPENDIX A

ACOUSTICS OF A PARTIALLY SATURATED POROUS MEDIUM

The purpose of this appendix is to highlight the main conceptual steps involved in the derivation of the complex-valued effective bulk modulus of the gas phase $K_g(\omega)$. To simplify the notation, the tilde above functions and quantities in the frequency domain is omitted. The tilde above density terms and tortuosity is used to denote the frequency-dependent nature of these functions (see Allard, 1993).

Let us consider a spherical gas bubble immersed in a fully liquid-saturated porous medium in the presence of an external oscillating pressure field. First, we focus on the external domain (fully water-saturated porous medium outside the bubble). We introduce the displacement potentials Φ_{c1} and Φ_{c2} associated with the fast wave and the slow compressional wave as follows:

$$\mathbf{u} = \nabla \Phi_{c1} + \nabla \Phi_{c2}, \tag{A-1}$$

and

$$\mathbf{U} = G_{c1}\nabla \Phi_{c1} + G_{c2}\nabla \Phi_{c2}, \tag{A-2}$$

where

$$G_{c1} = \frac{P - v_{c1}^2\tilde{\rho}_{11}}{v_{c1}^2\tilde{\rho}_{12} - Q}, \tag{A-3}$$

and

$$G_{c2} = \frac{P - v_{c2}^2\tilde{\rho}_{11}}{v_{c2}^2\tilde{\rho}_{12} - Q}. \tag{A-4}$$

In the above equations, $\mathbf{u}$ is the solid displacement, $\mathbf{U}$ is the fluid displacement, and v_{c1} and v_{c2} refer to the frequency-dependent wave velocities of the fast wave and the slow wave, respectively. Within the framework of Biot's theory, P and Q are the so-called generalized elastic coefficients, and $\tilde{\rho}_{11}$, $\tilde{\rho}_{12}$ are the effective density terms. For detailed expressions, we refer to the original papers of Biot (1956a, b) or classical books in the topic (Allard, 1993; Bourbié et al., 1987).

By assuming an $e^{i\omega t}$ temporal variation, the linearized radial momentum equation for the liquid phase can be written as follows:

$$\omega^2\phi\rho_f U_r = \phi\frac{\partial p_f}{\partial r} + (\tilde{\alpha}(\omega) - 1)\omega^2\phi\rho_f(u_r - U_r), \tag{A-5}$$

where ω is the angular frequency, ϕ is the porosity, ρ_f is the effective fluid density, p_f is the pressure, and $\tilde{\alpha}(\omega)$ is the frequency-dependent tortuosity according to the model of Johnson et al. (1987). The subscript r indicates the radial component of the displacement vector. Equation A-5 is integrated from the bubble radius ($r = a$) to infinity to find an equation of motion for the bubble, which reads

$$\begin{aligned}\phi\rho_f\omega^2(G_{c1}\Phi_{c1a} + G_{c2}\Phi_{c2a}) \\ = -\phi(p_{f\infty} - p_{fa}) + \omega^2\phi\rho_f(\tilde{\alpha}(\omega) - 1) \\ \times[\Phi_{c1a}(1 - G_{c1}) + \Phi_{c2a}(1 - G_{c2})].\end{aligned} \tag{A-6}$$

We seek solutions for potentials outside the bubble in the form

$$\Phi_{c1} = \frac{A_{c1}e^{-ik_1 r}}{r} \tag{A-7}$$

and

$$\Phi_{c2} = \frac{A_{c2}e^{-ik_2 r}}{r}, \tag{A-8}$$

where k_1 and k_2 are radial wavenumbers associated with the fast compressional wave and the slow compressional wave, respectively. Then, substitution of the solutions given by equations A-7 and A-8 into equation A-6, leads to the momentum equation in terms of two unknowns A_{c1} and A_{c2}. Boundary conditions at the bubble surface provide the remaining relationship to close the problem. Inside the bubble, we neglect the interaction between the gas and the solid matrix. The matrix is considered acoustically compact. It can be shown that this condition implies that the velocity of the solid phase linearly depends on r. We assume continuity of the radial velocity of the solid phase and its radial derivative across the bubble surface. This last condition allows a closed analytical solution and is consistent with numerical calculations based on the gas-pocket model (Dutta and Ode, 1979a, b). This procedure leads to the following relationship:

$$\frac{\partial^2 u_r}{\partial r \partial t}(a^+) = \frac{1}{r}\frac{\partial u_r}{\partial t}(a^+), \tag{A-9}$$

which holds at the outside of the bubble (a^+). The continuity of fluid volume provides an equation for the change in volume of the gas bubble ΔV_g in terms of the fluid and solid displacements at the bubble surface:

$$\Delta V_g = 4\pi a^2[(1-\phi)u_r + \phi U_r]. \tag{A-10}$$

We consider that the pressure difference across the bubble surface is balanced by the radial viscous stress in the fluid at the bubble surface:

$$p_f(a^+) - p_g = \frac{4}{3}\eta\frac{\partial^2 U_r}{\partial r \partial t}(a), \tag{A-11}$$

where $p_f(a^+)$ denotes the pressure outside the bubble evaluated at the bubble radius, p_g is the gas pressure inside the bubble, and η the fluid viscosity.

Substitution of the expressions for Φ_{c1} and Φ_{c2} in the boundary conditions (equations A-9-A-11), followed by some algebraic manipulations, leads to the following relationship between the volume of the gas bubble and the external pressure $p_{f\infty}$:

$$\omega^2\rho_f\left[\frac{a_1b_2 - a_2b_1}{a_1c_2 - a_2c_1} + \frac{4}{3}\frac{i\eta\phi a_1a_2(G_{c2}-G_{c1})}{\omega\rho_f(a_1c_2 - a_2c_1)}\right]\frac{V_g}{4\pi\phi a} = p_{f\infty} - p_g \tag{A-12}$$

where

$$a_j = k_j^2\left(1 - 3\frac{1+ik_ja}{k_j^2a^2}\right), \tag{A-13}$$

$$b_j = \phi G_{cj} - (G_{cj}-1)\frac{\tilde{\rho}_{12}}{\rho_f}, \tag{A-14}$$

and

$$c_j = (1+ik_ja)(1-\phi+\phi G_{cj}). \tag{A-15}$$

The last dissipative mechanism considered in this model is the thermal damping. It arises from the heat exchange between the gas phase and the solid matrix induced by oscillations of the bubble. Its contribution to the bulk modulus of the gas phase can be expressed as np_g. Here, we have introduced a complex-valued polytropic coefficient n:

$$n = \gamma\left[1 + 3(\gamma-1)\left[\frac{\coth(\psi(8\alpha_\infty\kappa_0/\phi)^{1/2})}{\psi(8\alpha_\infty\kappa_0/\phi)^{1/2}} - \frac{1}{(\psi(8\alpha_\infty\kappa_0/\phi)^{1/2})^2}\right]\right]^{-1}, \tag{A-16}$$

where $\psi = (1+i)(\omega/2a_g)$, a_g is the thermal diffusivity of the gas, γ is the specific heat ratio of the gas (for air $\gamma = 1.4$), κ_0 is the steady-state permeability, and α_∞ is the high-frequency limit of tortuosity. Champoux and Allard (1991) and Henry et al. (1995) reported a slightly different expression for the polytropic exponent n.

Finally, the following expression is found for the frequency-dependent effective bulk modulus of the gas phase $K_g = -V_g(\partial V_g/\partial p_{f\infty})^{-1}$:

$$K_g(\omega) = \frac{1}{3}a^2\omega^2\rho_f\left(\frac{3np_g}{a^2\omega^2\rho_f} - \frac{a_1b_2 - a_2b_1}{a_1c_2 - a_2c_1} - \frac{4}{3}\frac{i\eta\phi a_1a_2(G_{c2}-G_{c1})}{\omega\rho_f(a_1c_2 - a_2c_1)}\right). \tag{A-17}$$

REFERENCES

Allard, J. F., 1993, Propagation of sound in porous media: Elsevier Science Publ. Co., Inc.

Archie, G. E., 1942, The electrical resistivity log as an aid in determining some reservoir characteristics: Trans AIME, 146, **54–62**.

Biot, M. A., 1956a, Theory of propagation of elastic waves in a fluid-saturated porous solid, Part I: Low frequency range: Journal of the Acoustical Society of America, **28**, 168–178.

———, 1956b, Theory of propagation of elastic waves in a fluid-saturated porous solid, Part II: Higher frequency range: Journal of the Acoustical Society of America, **28**, 179–191.

Bourbié, T., O. Coussy, and B. Zinszner, 1987, Acoustics of porous media: Gulf Publ. Co.

Carcione, J. M., H. B. Helle, and N. H. Pham, 2003, White's model for wave propagation in partially saturated rocks: Comparison with poroelastic numerical experiments: Geophysics, **68**, 1389–1398.

Champoux, Y., and J. F. Allard, 1991, Dynamic tourtuosity and bulk modulus in air-saturated porous media: Journal of Applied Physics, **70**, 1975–1977.

Chao, G., D. M. J. Smeulders, and M. E. H. van Dongen, 2004, Shock-induced borehole waves in porous formations: Theory and experiments: Journal of the Acoustical Society of America, **116**, 693–702.

———, 2006a, Dispersive surface acoustic waves along partially saturated porous media: Journal of the Acoustical Society of America, **119**, 1347–1355.

———, 2006b, Measurements of shock-induced guided and surface acoustic waves along boreholes in poroelastic materials: Journal of Applied Physics, **99**, 094904.

Cheng, C. H., M. N. Toksoz, M. E. Willis, 1982, Determination of in situ attenuation from full waveform acoustic logs: Journal of Geophysics Research, **87**, 5477–5484.

Clavier, C., G. Coates, and J. Dumanoir, 1984, Theoretical and experimental bases for the dual-water model for interpretation of shaley sands: Society Petroleum Engineering Journal, **24**, 153–168.

Deresiewicz, H., and R. Skalak, 1963, On uniqueness in dynamic poroelasticity: Bulletin of the Seismology Society of America, **53**, 783–788.

Dutta, N. C., and H. Ode, 1979a, Attenuation and dispersion of compressional waves in fluid-filled porous rocks with partial gas saturation (White model) — Part I: Biot theory: Geophysics, **44**, 1777–1788.

———, 1979b, Attenuation and dispersion of compressional waves in fluid-filled porous rocks with partial gas saturation (White model) — Part II: Results: Geophysics, **44**, 1789–1805.

Feng, S., and D. L. Johnson, 1983, High-frequency acoustic properties of a fluid/porous solid interface. I: New surface mode: Journal of the Acoustical Society of America, **74**, 906–914.

Gubaidullin, A. A., O. Y. Kuchugurina, D. M. J. Smeulders, and C. J. Wisse, 2004, Frequency-dependent acoustic properties of a fluid/porous solid interfce: Journal of the Acoustical Society of America, **116**, 1474–1980.

Han, D. H., and M. Batzle, 1997, Fluid invasion effects on sonic interpretation: 67th Annual International Meeting, SEG, Expanded Abstracts, 198–300.

Hearst, J. R., P. H. Nelson, and F. L. Paillett, 2000, Well logging for physical properties: A handbook for geophysicists, geologists, and engineers: John Wiley & Sons Ltd.

Henry, M., P. Lemarinier, J. F. Allard, J. L. Bonarder, and A. Gedeon, 1995, Evaluation of the characteristic dimensions for porous sound-absorbing materials: Journal of Applied Physics, **77**, 17–20.

Johnson, D. L., J. Koplik, and R. Dashen, 1987, Theory of dynamic permeability and tortuosity in fluid-saturated porous media: Journal of Fluid Mechanics, **176**, 379–402.

Liu, H. L., 1988, Borehole modes in a cylindrical fluid-saturated permeable medium: Journal of the Acoustical Society of America, **84**, 424–431.

Liu, H. L., and D. L. Johnson, 1997, Effects of an elastic membrane on tube waves in permeable formations: Journal of the Acoustical Society of America, **101**, 3322–3329.

Paillet, F. L., and C. H. Cheng, 1991, Acoustic waves in boreholes — The theory and application of acoustic full-waveform logs: CRC Press.

Pride, S. R., J. G. Berryman, and J. M. Harris, 2004, Seismic attenuation due to wave-induced flow: Journal of Geophysical Research, **109**, B01201.

Pride, S. R., J. Harris, D. L. Johnson, A. Mateeva, K. Nihei, J. R. L. Nowack, J. R. Rector, H. Spetzler, R. Wu, T. Yamomoto, J. Berryman, and M.

Fehler, 2003, Permeability dependence of seismic amplitudes: The Leading Edge, **22**, 518–525.
Rosenbaum, J. H., 1974, Synthetic microseismograms: Logging in porous formations: Geophysics, **39**, 14–32.
Schmitt, D. P., 1988, Effects of radial layering when logging in saturated porous formations: Journal of Acoustical Society of America, **84**, 2200–2214.
Schmitt, D. P., M. Bouchon, and G. Bonnet, 1988, Full-wave synthetic acoustic logs in radially semiinfinite saturated porous media: Geophysics, **53**, 807–823.
Sen, P. N., and P. A. Goode, 1988, Shaley sand conductivities at low and high salinities: 29th Annual Logging Symposium. Transactions of the Society of Professional Well Log Analysts.
Sinha, B., and S. Asvadurov, 2004, Dispersion and radial depth of investigation of borehole modes: Geophysical Prospecting, **52**, 271–286.
Smeulders, D. M. J., and M. E. H. van Dongen, 1997, Wave propagation in porous media containing a dilute gas-liquid mixture: Theory and experiments: Journal of Fluid Mechanics, **343**, 351–373.
Tang, X. M., 1994, Effects of mudcake on the measurement of fluid flow properties using borehole acoustic waves: 64th Annual International Meeting, SEG, Expanded Abstracts, 78–81.
Tang, X. M., and A. Cheng, 2004, Qualitative borehole acoustic methods: Elsevier Science Publ. Co., Inc.
Tang, X. M., and C. H. Cheng, 1996, Fast inversion of formation permeability from Stoneley wave logs using a simplified Biot-Rosenbaum model: Geophysics, **61**, 639–645.
Taylor, S. R., and R. J. Knight, 2003, An inclusion-based model of elastic wave velocities incorporating patch-scale fluid pressure relaxation: Geophysics, **68**, 1503–1509.
Tichelaar, B. W., H.-L. Liu, and D. L. Johnson, 1999, Modeling of borehole Stoneley waves in the presence of skin effects: Journal of the Acoustical Society of America, **105**, 601–609.
Waxman, M. H., and L. J. M. Smits, 1968, Electrical conduction in oil bearing shaly sands: Society of Petroleum Engineers Journal, **8**, 107–122.
White, J. E., 1975, Computed seismic speeds and attenuation in rocks with partial gas saturation: Geophysics, **40**, 224–232.
———, 1983, Underground sound-application of seismic waves: Elsevier Science Publ. Co., Inc.
Winkler, K. W., H.-S. Liu, and D. L. Johnson, 1989, Permeability and borehole stoneley waves: Comparison between experiment and theory: Geophysics, **54**, 66–75.
Wood, A. B., 1955, A textbook of sound: Bell.